A homozygous ATAD1 mutation impairs postsynaptic AMPA receptor trafficking and causes a lethal encephalopathy

Juliette Piard[1#], George K. Essien Umanah[2, 3#], Frederike Harms[4#], Leire Abalde-Atristain[2,5], Daniel Amram[6], Melissa Chang[2,3], Malik Alawi[4], Vincenzo Salpietro-Damiano[7], Mark I Rees[8], Henry Houlden[7], Ted M. Dawson[2,3,4,9,10], Valina L. Dawson[2,3,4,9,11##], Lionel Van Maldergem[1##] and Kerstin Kutsche[5##]

1- Centre de génétique humaine, Université de Franche-Comté, Besançon, France
2- Neuroregeneration and Stem Cell Programs, Institute for Cell Engineering, Johns Hopkins University School of Medicine, Baltimore, MD 21205, USA
3- Department of Neurology, Johns Hopkins University School of Medicine, Baltimore, MD 21205, USA
4- Institut für Humangenetik, Universitätsklinikum Hamburg-Eppendorf, Hamburg, Germany
5- Cellular and Molecular Medicine Graduate Program, Johns Hopkins University School of Medicine, Baltimore, MD 21205, USA
6- Unité fonctionnelle de génétique Clinique, Centre hospitalier intercommunal, Créteil, France
7- Department of Molecular Neuroscience, UCL Institute of Neurology , London, UK
8- Institute of Life Sciences, Swansea University Medical School, Swansea University, Swansea, UK
9- Solomon H. Snyder Department of Neuroscience, Johns Hopkins University School of Medicine, Baltimore, MD 21205, USA
10- Department of Pharmacology and Molecular Sciences, Johns Hopkins University School of Medicine, Baltimore, MD 21205, USA
11- Department of Physiology, Johns Hopkins University School of Medicine, Baltimore, MD 21205, USA

#equally contributing first authors
###equally contributing last/senior authors

Corresponding author: L. Van Maldergem

Abstract

Members of the AAA+ superfamily of ATPases are involved in the unfolding of proteins and disassemby of protein complexes and aggregates. *ATAD1* encoding the ATPase family, AAA+ domain containing 1-protein Thorase, maintains the function and integrity of mitochondrial and peroxisomes. Postsynaptically Thorase controls the internalization of excitatory, glutamatergic AMPA receptors (AMPAR) by disassembling complexes between the AMPAR-binding protein, GRIP1, and the AMPAR subunit GluA2. Here we identify a homozygous c.1070_1071delAT frameshift mutation in *ATAD1* by whole exome sequencing in three siblings born to consanguineous parents who presented with severe and lethal encephalopathy with stiffness and arthrogryposis. Biochemical and cellular analyses show that the 2-pb deletion in *ATAD1* strongly impacts the oligomeric state of Thorase, reduces the stability or expression of some golgi, peroxisomal and mitochondrial proteins, affects disassembly of AMPAR and Thorase oligomer complexes and displays reduced GluA2 surface expression. Taken together, our molecular and functional analyses identify Thorase hyperactivity *ATAD1* deficiency as a new cause of severe encephalopathy.

Introduction

The AAA+ family, is a large enzymatic group of ATPases associated with various cellular activities that induce conformational changes in a wide range of substrate proteins. These ATPases have been involved in various human diseases such as peroxisome biogenesis disorders, early-onset torsion dystonia linked to *DYT1, SPG4* and *PG7*-related hereditary spastic paraplegia or a specific form of inclusion-body myopathy. One of them, the AAA+ ATPase Thorase encoded by *ATAD1* plays a critical role in regulating the surface expression of AMPAR (a-amino-3-hydroxy-5-methylisoxazole-4-proprionate receptors) thus regulating synaptic plasticity, learning and memory. Here, we report the genotype-phenotype relationships in three infants exhibiting severe lethal encephalopathy with stiffness and athrogryposis resulting from an activating *ATAD1* mutation.

Results and discussion

Siblings with severe encephalopathy and a homozygous ATAD1 mutation. Parents are first cousins originating from southern Tunisia (Figure 1A). The three siblings were born at term by c-section for fetopelvic disproportion with normal growth parameters. Pregnancies were marked by maternal diabetes. The first patient (patient 1; IV: 1) is a male who presented at birth with respiratory distress requiring assisted ventilation. Generalized hypertonia with an abnormal startle reflex, adducted thumbs, spontaneous tremor and clonic movements were observed from day 1. EEG showed altered background with slow and disorganized activity and multiple multifocal epileptic discharges. Examination at two months showed major stiffness and distal arthrogryposis with fixed prone position of upper limbs and bilateral camptodactyly. Deep tendon reflexes were brisk with extensor plantar reflex. Visual contact was absent and narrow myosis unresponsive to light was noted. Inexpressive facies, anteverted nares, high arched palate and brachycephaly were observed. Kyphoscoliosis and benign umbilical hernia were also noted. He had several episodes of pneumonia. He died after multiple organ failure at the age of 5 months. Abdominal ultrasound, eye fundus, spinal cord and brain MRI were normal. Skeletal X-rays indicated dorsal scoliosis. A large metabolic screening and array-CGH did not show any abnormality. A muscle biopsy was performed and showed focal atrophy of both fiber types with grouping suggestive of a neurogenic disorder. His younger brother (patient 2; IV: 2) presented at birth with respiratory distress, poor spontaneous mobility and no visual contact. Examination showed generalized hypertonia with transient tremor, bilateral adducted thumbs and clenched toes. He underwent surgery for bilateral inguinal hernia at 2 months. Regular swallowing difficulties resulted in food misrouting accidents with subsequent pneumonia. By contrast to his brother, a few intentional smiles were noted before death after a novel episode of

aspiration pneumonia at the age of 3 months. The ultrasound follow-up of the third pregnancy indicated decreased fetal movements during the third trimester. The girl (patient 3; IV: 3) presented at birth with transient respiratory distress requiring assisted ventilation. In her case, axial hypotonia contrasted with limb hypertonia. Examination showed poor spontaneous mobility, distal arthrogryposis with adductus thumbs, ulnar deviation and bilateral clubfoot. Eye contact was present. She had gastro-esophageal reflux. Brain MRI performed at day 1 showed myelination delay and a periventricular white matter hypersignal. EEGs were normal. She died at the age of 6 months.

The clinical picture of the oldest sibling (patient 1) overlapped with hyperekplexia (MIM 149400), which is characterized by generalized stiffness after birth that normalizes during the first years of life, increased muscle tone (hypertonia) and an exaggerated startle reaction to unexpected stimuli (1). Mutations in *GLRA1* and *SLC6A5* account for the majority of cases affected by this neurological disorder (2). Sanger sequencing of these two genes and *SCN4A*, in which mutations cause congenital paramyotonia (MIM 168300) and muscle stiffness (3), performed in patient 1 failed to identify any pathogenic mutation. Next, we performed whole-exome sequencing (WES) in two affected siblings, patients 1 and 3, and their healthy mother (Figure 1A). Analysis of the WES data was performed according to an autosomal recessive model, owing to parental consanguinity. We identified six rare variants in the homozygous state (with an allele frequency <0.5% in population databases [dbSNP138, 1000 Genomes Project, Exome Variant Server, and ExAC Browser] and no homozygous carriers in the ExAC Browser) shared by the two affected siblings and present in the heterozygous state in their healthy mother (Supplemental Table S1). Three of these variants were excluded to underlie the phenotype in the three siblings through segregation analysis in the entire family (Supplemental Table S2). The remaining three variants in *RNLS*, *CDH8* and *ATAD1* are not located within a region of significant homozygosity as assessed by homozygosity mapper (4), but *RNLS* and *ATAD1* were located in a homozygous region of ~1.3

Mb on chromosome 10 (data not shown). In silico pathogenicity assessment and splice site tools predicted that the missense variant p.(Ile114Val) in *RNLS* and the synonymous variant c.726T>C in *CDH8* do not have a deleterious effect on protein function (Supplemental table S3) nor does it alter splicing of the pre-mRNA (Supplemental table S4). In contrast, the 2-bp deletion c.1070_1071delAT in the last exon of *ATAD1* was predicted to result in a frameshift and addition of 14 ATAD1-unrelated amino acid residues at the C-terminus [p.(His357Argfs*15)], with a potential damaging effect on protein function (Figure 1 and Supplemental Table S3). The c.1070_1071delAT variant represents a very rare *ATAD1* allele, as it was absent in the gnomAD Browser (in 251,868 alleles; data not shown) and had an allele frequency of 8.266e-06 in the ExAC Browser (1 heterozygote in 120,978 alleles; Supplemental Table S1) that is in accordance with the rarity of the neurological disorder in the three siblings. *ATAD1* mRNA analysis from patient-derived fibroblasts demonstrated the presence of transcripts harboring the 2-bp deletion at their 3' end (Figure 1B), indicating that mutated *ATAD1* mRNAs escape nonsense-mediated mRNA decay and likely produces a protein with an altered C-terminal end.

ATAD1 encodes the ATPase family, AAA+ domain containing 1-protein, Thorase that is highly expressed in mouse brain and testis (5). Members of the AAA superfamily of ATPases are involved in the unfolding of proteins and disassembly of protein complexes and aggregates (6). In addition, Thorase is able to maintain mitochondrial function through degradation of mislocalized tail-anchored proteins to the outer mitochondrial membrane. These data indicate an important role of Thorase in maintaining mitochondrial function and integrity (7, 8). A similar function of Thorase has also been proposed for peroxisomes (9). Postsynaptically, Thorase controls the internalization of excitatory, glutamatergic AMPA receptors (AMPAR) by disassembling complexes between glutamate receptor interacting protein (GRIP1) and the AMPAR subunit GluA2. Accordingly, Thorase deficiency in mice leads to enhanced AMPAR density at the cell surface that results in enhanced excitatory postsynaptic currents and impaired adaption to excitatory stimuli. Although homozygous Thorase knockout mice are viable and do not show any obvious gross malformations,

approximately 80% die of a seizure-like syndrome (5). The C-terminus of Thorase is evolutionarily highly conserved (Supplemental Figure S1) and involved in intra- and intermolecular contacts of oligomerized AAA+-ATPase complexes (9). As the *ATAD1* mutation found in the three siblings with severe encephalopathy deletes the last five residues of the C-terminus and adds 14 novel amino acids (Figure 1B and Supplemental Figure 1), we assumed it might lead to a gain-of-function of Thorase C-terminal end. Functional studies were in accordance with this view.

Replication studies. Two different cohorts of patients were studied. First, 2000 WES from epileptic encephalopathies and hyperekplexia patients were screened. Then, 27 cases of hyperekplexia (negative for known genes) with parental consanguinity or atypical phenotype with severe developmental outcomes were Sanger sequence-screened. No deleterious mutation in *ATAD1* was identified. The present results suggest that *ATAD1*-related congenital encephalopathy with stiffness is an extremely rare condition.

Altered protein expression but functional mitochondria in 2-bp deletion patient fibroblasts. *ATAD1* mRNA analysis from patient-derived fibroblasts suggested that the mutated *ATAD1* mRNAs produce a protein with an altered C-terminal end. We examined the expression of *ATAD1* in patient fibroblasts via immunoblotting analyses, which confirmed that the 2bp-deletion ATAD1 protein mutant is expressed in the patients (Figure 2A). Previous studies showed that the deletion of *ATAD1* causes accumulation of peroxisomal biogenesis factor 26 (PEX26) and golgi SNARE 28 kDa (GOS28) in human cell lines [2]. In patient cells expressing mutant Thorase, protein expression levels of PEX26 and GOS28 were significantly lower compared to control cells (Figures 2A and 2B). In addition, cytochrome c oxidase subunit 1 (COX1), hexokinase 1 and 2 (HXK1 and 2), and voltage dependent anion channel 1 (VDAC1) were reduced while the translocase of outer mitochondrial membrane 20 (TOMM20) were not altered. Staining the patient and control cells with GOS28 and PEX26 to evaluate the

distribution of Golgi and peroxisomal proteins, respectively, supported our previous observation by immunoblot that their levels are decreased in patient cells when compared to healthy controls (Figure 2C). Thus, the 2-bp deletion in Thorase affects the stability or expression of GOS28 and PEX26. Interestingly, patient fibroblasts exhibit normal tubular mitochondrial morphology when labeled with an antibody for the mitochondrial protein TOMM20 (Figure 2C) consistent with the immunoblot results. The patient fibroblasts also exhibit efficient mitochondrial respiration (7, 12) similar to wild type cells (Figure 2D). These results suggest that the 2-bp deletion has no significant effect on mitochondrial function despite the reduction in the level of some mitochondrial proteins.

Thorase 2-bp deletion (CT mutant) affects the oligomer state of Thorase but causes no defects in its ATPase activity. The predicted 3D model of Thorase suggests that the 2-bp deletion in *ATAD1* results in changes in the secondary structure at the C-terminus of Thorase (Figure 2E). The wild type C-terminus (Ala349-Asp361) is predicted to form a helix, while the 2-bp deletion mutant the helix is shortened and sandwiched by 2 loops to form a Loop-Helix-Loop (LHL) structure. To further examine the activity of the *ATAD1* 2-bp deletion mutant, a recombinant expression vector encoding for it was generated (hereinafter referred to as Thorase-CT mutant). Purified wild type (WT) Thorase elutes as 70 kD (dimer) on a size-exclusion column, while the CT mutant elutes at a higher molecular weight >400 kD (Figure 2F). Thus, the 2-bp deletion seems to lock the CT mutant in an oligomeric state. Both WT and CT migrate at approximately 36 kD by SDS-PAGE as indicated by Coomassie staining or immunoblot analysis with an anti-Thorase antibody (Figure 2G). The CT mutant migrates higher than the WT due to the addition of 14 protein-unrelated amino acids to its C-terminus. ATP binding assessment using UV light-induced cross-linking (11) of radiolabeled

[α-P^{32}]ATP bound to purified recombinant proteins suggests that the CT mutant binds ATP similar to WT (Figure 2H and 2I). ATP hydrolysis is neither significantly affected in the CT mutant (Figure 2J). Taken together, the 2-bp deletion in Thorase does not affect ATPase activity but strongly impacts the oligomeric state of Thorase most likely as a result of the LHL formation at the C-terminus.

The Thorase-CT mutant has defects in the disassembly of AMPAR-GRIP1 and Thorase oligomer complexes. Since Thorase regulates AMPA receptor trafficking (5, 13), we examined Thorase 2-bp mutant (CT) interactions with and disassembly of GluA2-GRIP1 complex. Purified GST-Thorase WT or CT were immobilized on beads and mixed with Thorase KO (Thorase$^{-/-}$) whole brain lysates in the presence of ADP, ATP or ATPγS (Figures 3A to 3D). Both WT and CT bind efficiently to the GluA2-GRIP1 complex in the presence of non-hydrolyzable ATPγS, which maintains Thorase in the oligomeric substrate-bound state. However, in the presence of ATP (which can be hydrolyzed and is required for the proper disassembly of protein complexes by Thorase) Thorase WT disassembles the complex, whereas the disassembly is significantly impaired with Thorase CT (Figure 3D). These data suggest that the 2-bp deletion impairs Thorase-mediated AMPAR trafficking, likely by its inability to normally transition from the oligomeric to the monomeric state. The formation of oligomeric complexes by Thorase and other AAA ATPases is critical for their proper assembly and disassembly of protein complexes (14). Therefore, we determined whether the defect in AMPAR complex disassembly by the CT mutant is a result of defects in Thorase oligomer disassembly. Oligomeric formation and disassembly were evaluated by ATP binding and glutaraldehyde cross-linking of protein complexes as previously described (11). Purified Thorase samples were mixed with ATP (at 4 ^{O}C to prevent its hydrolysis or at 37 ^{O}C to allow

for its hydrolysis) or non-hydrolysable ATPγS (Figures 3E to 3G). In the presence of either ATP at 4 ^{O}C (ATP-4) or ATPγS Thorase forms large oligomeric complexes of molecular weights greater than 250 kDa. While about 75% of Thorase WT forms oligomer, 95% of Thorase CT was found in the oligomeric state. Upon ATP hydrolysis (ATP-37), about 80% of Thorase WT and 65% of Thorase CT oligomeric complexes disassemble (Figure 3G). These results indicate and further confirm that the 2-bp deletion impairs the normal disassembly of Thorase oligomers.

Thorase 2-bp deletion mutant displays reduced GluA2 surface expression. Since Thorase mediates surface expression of AMPARs the effects of the 2-bp deletion on AMPARs trafficking was evaluated. An antibody feeding internalization assay for endocytosis of surface GluA2 receptors (5, 13) was performed in Thorase KO primary cortical neurons transduced with lentiviral WT or CT mutant GFP-tagged Thorase. Live neurons were incubated with an anti-GluA2 N-terminal antibody followed by induction of GluA2 endocytosis with N-Methyl-D-aspartate (NMDA) (20 μM) and glycine (10 μM). In control unstimulated Thorase CT cultures there is decreased surface expression of GluA2 compared to Thorase WT cultures (Figures 3H and 3I). In contrast, the ratio of surface GluA2/intracellular GluA2 in NMDA- and glycine-stimulated Thorase CT cortical cultures remains similar to that of stimulated Thorase WT cultures (Figures 3J and 3K). Thus, the 2-bp deletion mutant neurons exhibit significantly reduced surface GluA2 only under unstimulated conditions. To further evaluate the effects of the 2-bp deletion mutation in Thorase on AMPAR trafficking, GluA2 surface expression was assessed by a bis(sulfosuccinimidyl)-suberate (BS3) cross-linking assay that allows for the quantification of both surface and intracellular receptor pools (15). The results suggest decreased levels of

surface GluA2 in unstimulated CT cultures compared to WT cultures (Figures 3L and 3M). In response to NMDA there is no significant differences in internalization of surface GluA2 in cultures compare to WT cultures. The results suggest that the Thorase 2-bp deletion mutant may inhibit the reinsertion of AMPARs back to the surface following endocytosis.

Here, we describe a gain-of-function mutation in *ATAD1* that causes severe lethal encephalopathy with stiffness and athrogryposis in infants as a result of a deficiency in AMPAR recycling and unstable protein expression. Previously, we reported a loss-of-function mutation in ATAD1 that causes hypertonia, seizures, respiratory failure and death (PMID: 28180185). Given that different ATAD1 mutations have been identified in two separate families with critical clinical phenotypes in infants, ATAD1 can be considered as a very important human disease-causing gene. The gain-of-function mutation in *ATAD1* decreases the population of excitatory postsynaptic AMPA receptors. AMPAR receptor surface expression is a known pathogenic mechanism in encephalopathy; for example, decreases in extrasynaptic AMPAR expression impairs synaptic plasticity in a model of hepatic encephalopathy (PMID: 26363416). There are likely to be other targets of Thorase that contribute to the encephalopathy and neurologic phenotype of patients with Thorase mutations. Consistent with this notion is the observation that the AMPAR antagonist, perampanel only partially rescued the phenotype of patients with a loss of function muation in *ATAD1* (PMID: 28180185). The findings establish an important avenue for clinicians to examine the role of *ATAD1* mutations in several neurological diseases with unknown cause.

Altogether, these results indicate that a homozygous frameshift mutation in *ATAD1* results in a severe and lethal encephalopathy with stiffness and arthrogryposis. Interestingly, through a rare gain-of-function effect, an unusual mechanism in autosomal recessive disease, production of an altered protein with a novel function of the C-terminal end was correlated with a major congenital stiffness that differs from hyperekplexia by its major neurological impairment. The strong impaction on AMPAR trafficking is likely to result in a generalized post-synaptic excitatory state in accordance with the clinical picture. By contrast, mitochondrial function and ATPase activity does not seem to suffer major changes, with the methods used. Replication studies failed to identify new cases suggesting *ATAD1*-related congenital encephalopathy is an extremely rare condition.

Authors contribution

LVM and KK designed the study. GKU, LA, MC, FH, performed experiments. MR, HH and VSD investigated a replication cohort. JP, KK, LVM and GKU wrote the manuscript. VLD and TMD supervised the biochemical and cell biologic studies and edited the manuscript. All authors approved the final manuscript.

References

1. Tijssen MAJ, and Rees MI. In: Pagon RA, Adam MP, Ardinger HH, Wallace SE, Amemiya A, Bean LJH, Bird TD, Ledbetter N, Mefford HC, Smith RJH, et al. eds. *GeneReviews(R)*. Seattle (WA): University of Washington, Seattle University of Washington, Seattle. GeneReviews is a registered trademark of the University of Washington, Seattle. All rights reserved.; 1993.
2. Carta E, Chung SK, James VM, Robinson A, Gill JL, Remy N, Vanbellinghen JF, Drew CJ, Cagdas S, Cameron D, et al. Mutations in the GlyT2 gene (SLC6A5) are a second major cause of startle disease. *J Biol Chem.* 2012;287(34):28975-85.
3. Koch MC, Ricker K, Otto M, Grimm T, Bender K, Zoll B, Harper PS, Lehmannhorn F, Rudel R, and Hoffman EP. Linkage Data Suggesting Allelic Heterogeneity for Paramyotonia-Congenita and Hyperkalemic Periodic Paralysis on Chromosome-17. *Hum Genet.* 1991;88(1):71-4.
4. Seelow D, Schuelke M, Hildebrandt F, and Nurnberg P. HomozygosityMapper--an interactive approach to homozygosity mapping. *Nucleic Acids Res.* 2009;37(Web Server issue):W593-9.
5. Zhang J, Wang Y, Chi Z, Keuss MJ, Pai YM, Kang HC, Shin JH, Bugayenko A, Wang H, Xiong Y, et al. The AAA+ ATPase Thorase regulates AMPA receptor-dependent synaptic plasticity and behavior. *Cell.* 2011;145(2):284-99.
6. Hanson PI, and Whiteheart SW. AAA+ proteins: have engine, will work. *Nat Rev Mol Cell Biol.* 2005;6(7):519-29.
7. Chen YC, Umanah GK, Dephoure N, Andrabi SA, Gygi SP, Dawson TM, Dawson VL, and Rutter J. Msp1/ATAD1 maintains mitochondrial function by facilitating the degradation of mislocalized tail-anchored proteins. *EMBO J.* 2014;33(14):1548-64.
8. Okreglak V, and Walter P. The conserved AAA-ATPase Msp1 confers organelle specificity to tail-anchored proteins. *Proc Natl Acad Sci U S A.* 2014;111(22):8019-24.
9. Grimm I, Erdmann R, and Girzalsky W. Role of AAA(+)-proteins in peroxisome biogenesis and function. *Biochim Biophys Acta.* 2016;1863(5):828-37.
10. Harvey RJ, Topf M, Harvey K, Rees MI. The genetics of hyperekplexia: more than startle! Trends Genet 2008;24:439-47.
11. Babst, M., et al., *The Vps4p AAA ATPase regulates membrane association of a Vps protein complex required for normal endosome function.* EMBO J, 1998. 17(11): p. 2982-93.
12. Cooper, O., et al., *Pharmacological rescue of mitochondrial deficits in iPSC-derived neural cells from patients with familial Parkinson's disease.* Sci Transl Med, 2012. 4(141): p. 141ra90.
13. Prendergast, J., et al., *Ganglioside regulation of AMPA receptor trafficking.* J Neurosci, 2014. 34(39): p. 13246-58.
14. Fujiki, Y., et al., *Dynamic and functional assembly of the AAA peroxins, Pex1p and Pex6p, and their membrane receptor Pex26p involved in shuttling of the PTS1 receptor Pex5p in peroxisome biogenesis.* Biochem Soc Trans, 2008. 36(Pt 1): p. 109-13.
15. Conrad, K.L., et al., *Formation of accumbens GluR2-lacking AMPA receptors mediates incubation of cocaine craving.* Nature, 2008. 454(7200): p. 118-21.

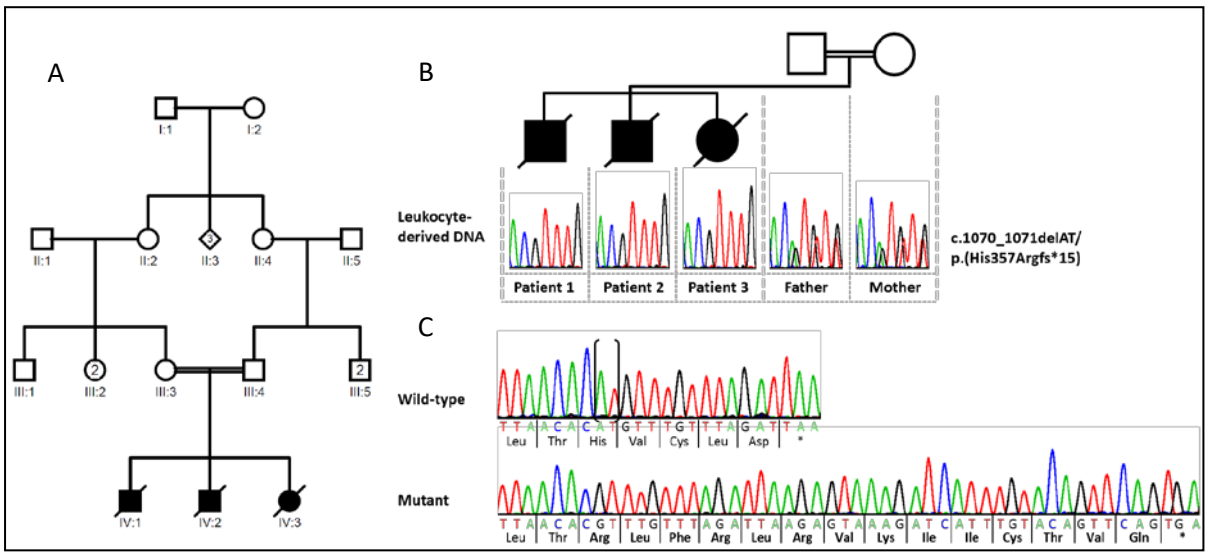

Figure 1. DNA and RNA analysis in the family with three siblings carrying the homozygous *ATAD1* mutation. (A) Pedigree of the family. (B) Partial sequence electropherograms demonstrating the *ATAD1* c.1070_1071delAT [p.(His357Argfs*15)] mutation in the homozygous state in leukocyte-derived DNA of the affected siblings (Patients 1, 2 and 3). Their healthy parents (Father and Mother) are heterozygous carriers of the mutation. (C) Partial sequence electropherograms show the 2-bp deletion in *ATAD1* in fibroblast-derived cDNA of one sibling (Mutant) in comparison to the cDNA sequence of a healthy individual (Wild-type). Deleted bases are marked by parenthesis in the normal sequence. The encoded amino acid residues are depicted below each sequence in the three-letter code and indicate the altered and extended C-terminus of ATAD1 (highlighted in bold). *: stop codon.

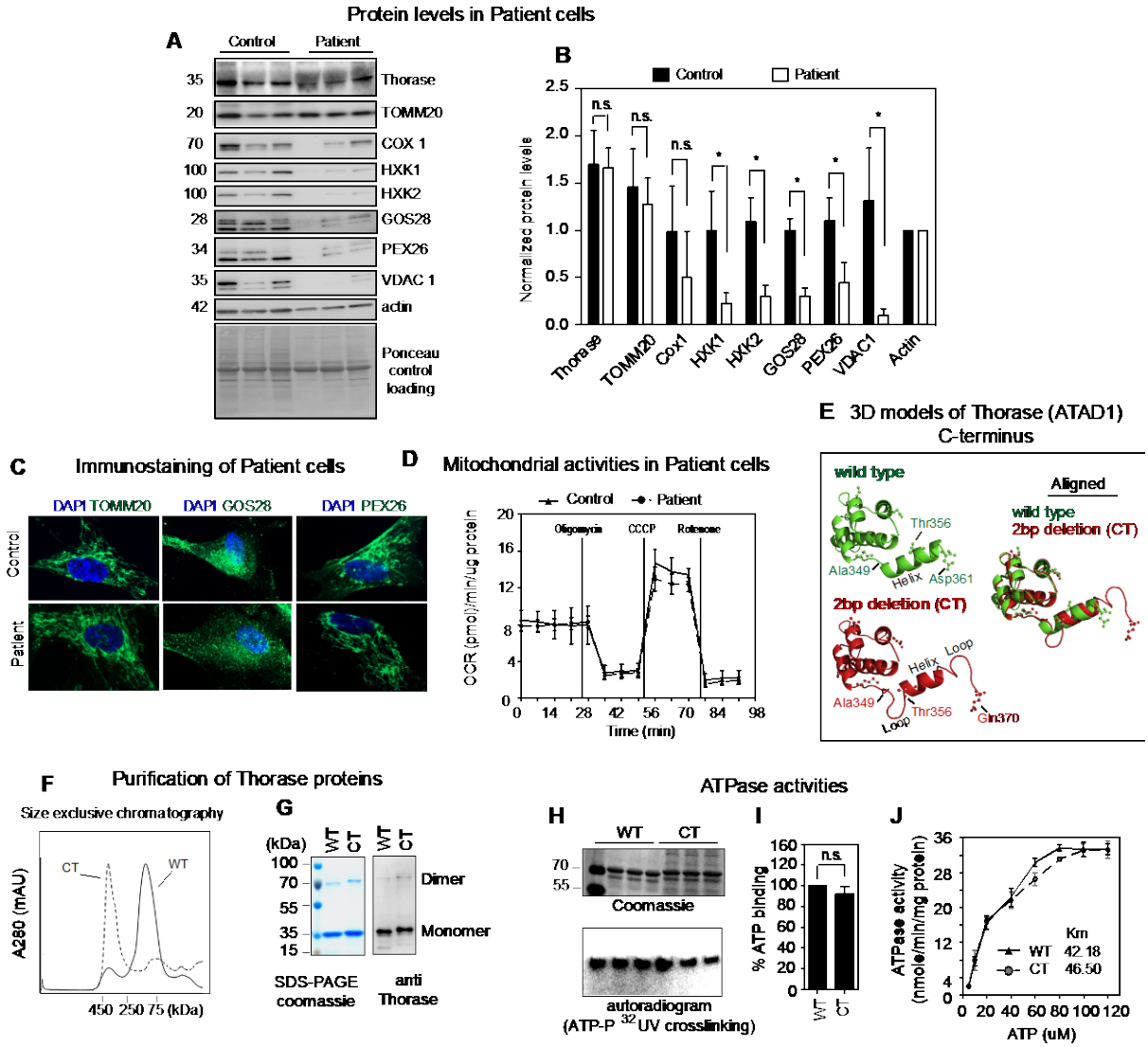

Figure 2. Protein levels altered in patient cells. (A) Immunoblots of lysates obtained from patient and control fibroblasts. COX1, cytochrome c oxidase subunit 1; GOS28, golgi SNARE 28 kDa; HXK1 and 2, hexokinase 1 and 2; PEX26, peroxisomal biogenesis factor 26; TOMM20, translocase of outer mitochondrial membrane 20; VDAC1, voltage dependent anion channel 1. (B) The optical densitometry quantification of (A). The values represent the mean+SEM (n=3, n.s. $p>0.05$, * $p<0.05$, two-way ANOVA, Tukey's multiple comparison tests). (C) Representative images of the mitochondrial morphology (TOMM20) of the control and patient fibroblasts. The cells were also stained for Golgi (GOS28), peroxisome (PEX26) and the nuclei with DAPI (blue). (D) Oxygen consumption rate (OCR) of the patient and control fibroblasts. The data was normalized to the amount of protein in each well and represents average from three independent experiments (n= 6 wells for each experiments). (E) Predicted 3D structure of Thorase wild type (green) and CT mutant (red). (F) Size exclusive

chromatograph profile of purified recombinant Thorase. WT Thorase appears as a dimer (~70 kDa), whereas the Thorase CT mutant appears as oligomer. (G) Purified proteins resolved on 10% SDS-PAGE stained with coomassie stain and immunoblotted with anti-Thorase antibody. (H) UV light-induced cross-linking of radiolabeled [α-P^{32}]ATP to purified proteins. The cross-linked proteins were separated on 10% SDS–PAGE. Upper panel is Coomassie stain of the protein input and lower panel is a representative of autoradiogram of [α-P^{32}]ATP bound to proteins. (I) Percent ATP bound to the Thorase in (H). (J) Analysis of ATP hydrolysis (ATPase) activities of purified Thorase. The Km (mM) values are shown on the graph. (mean ± standard error of the mean [SEM] of experiments performed in triplicate. n.s (not significant) $p > 0.10$, ANOVA with Tukey-Kramer post-hoc test when compared with WT).

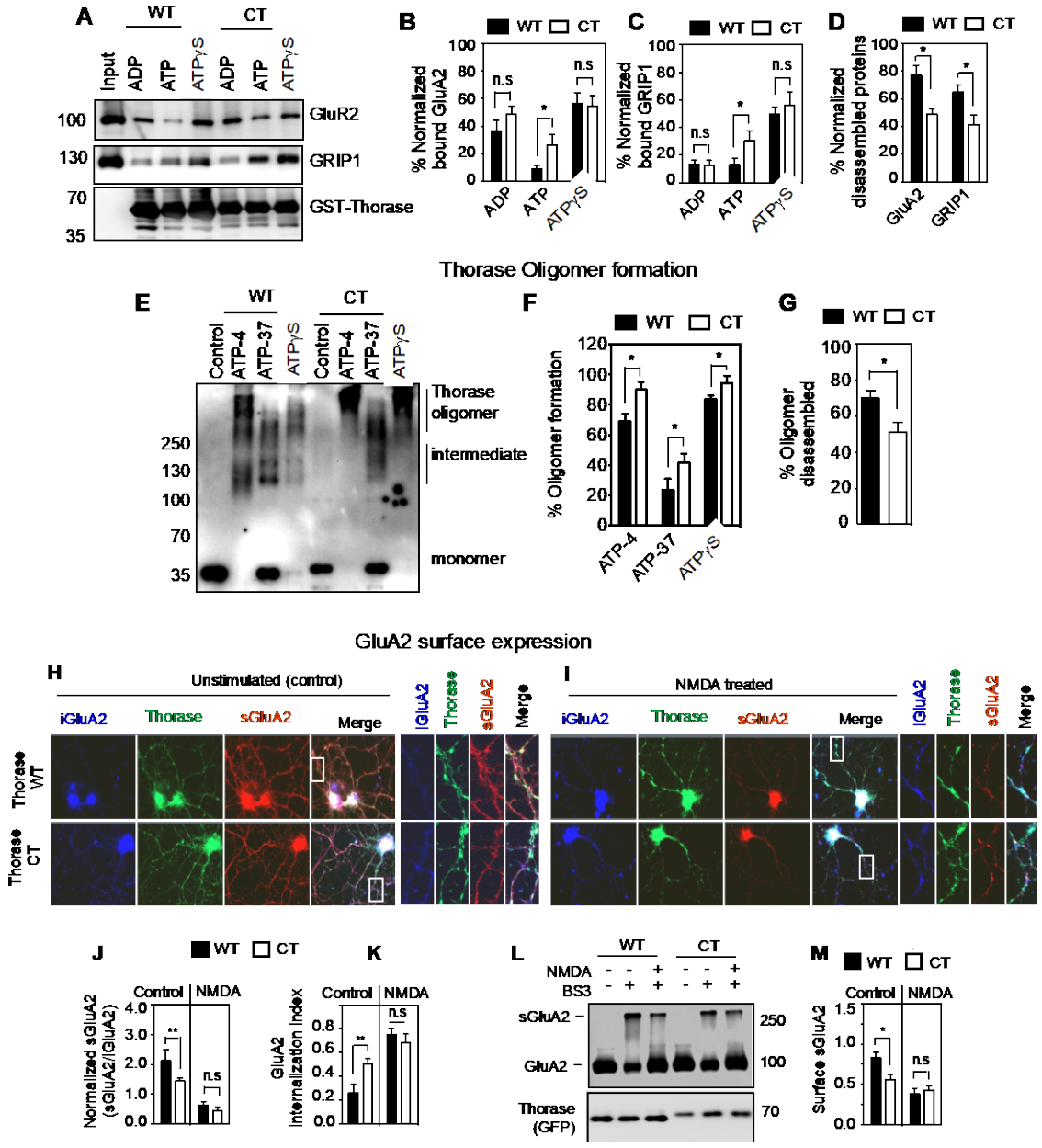

Figure 3. Thorase 2-bp deletion affects GluA2-GRIP1 complex disassembly and GluA2 surface expression. (A) Immunoblot analyses of GST-Thorase pulldown of the GluA2-GRIP1 complex from Thorase KO whole brain lysate in the presence of different nucleotides (ADP, hydrolysable ATP and non-hydrolysable ATPγS). The samples were incubated at 4 °C for binding and then at 37 °C for ATP hydrolysis to trigger the disassembly of the protein complex. (B-C) The graphs represents normalized percent bound GluA2 (B) and GRIP1 (C) in the GST-Thorase pulldown samples for (A). (D) Normalized percentage of GluA2 and GRIP1 disassembled from Thorase-GluA2-GRIP1 complex in (A). (E) Immunoblot analyses of Thorase WT and CT mutant oligomer formation. The samples were cross-linked by glutaraldehyde in the presence ATP or ATPγS. The ATP treated samples were treated at 4 °C

for binding (ATP-4) or at 37 ^{o}C (ATP-37) for ATP hydrolysis. (F) The graph represents normalized percent oligomer formed for (E). (G) The percentage of Thorase oligomer disassembled at 4 ^{o}C (mean ± standard error of the mean [SEM] of three experiments performed in triplicate. n = 3, **p < 0.05, *p < 0.10, n.s p > 0.10, ANOVA with Tukey-Kramer post-hoc test compared with WT, Power: 1-β err prob = 1.0) . (H-I) Representative images of unstimulated and NMDA-induced endocytosis of GluA2 in Thorase KO (-/-) neurons expressing Thorase-GFP wild type (WT) or 2-bp deletion (CT) mutant. (J) Normalized ratio of surface GluR2 (sGluR2) to internalized GluR2 (iGluR2) for (H-I). (K) GluA2 internalization index measured as the ratio of iGluR2 to the total GluR2 (iGluR2 plus sGluR2) fluorescence intensities. (L) Immunoblot analyses of BS3-crosslinking of sGluA2 in Thorase KO neurons expressing Thorase-GFP WT or CT mutant. (M) The normalized optical densitometry quantification of sGluR2 for (L). (mean ± standard error of the mean [SEM] of three experiments performed in triplicate. n = 3, **p < 0.05, *p < 0.10, n.s p > 0.10, ANOVA with Tukey-Kramer post-hoc test when compared with WT).